ELSEVIER

Catalysis Today 76 (2002) 291–300

CATALYSIS TODAY

www.elsevier.com/locate/cattod

The influence of different irradiation sources on the treatment of nitrobenzene

Miguel Rodriguez [b], Vitaliy Timokhin [c], Florian Michl [a], Sandra Contreras [a], Jaime Gimenez [a], Santiago Esplugas [a,*]

[a] *Department d'Enginyeria Quimica i Metal·lurgia, Universitat de Barcelona, Marti i Franques 1, 08028 Barcelona, Spain*
[b] *Universidad de Los Andes, Escuela Basica de Ingenieria, La Hechicera, Merida, Venezuela*
[c] *Department of Physical Chemistry, Institute of Physical Chemistry, National Academy of Sciences of Ukraine, 3a Naukova Street, 79053 Lviv, Ukraine*

Abstract

This work describes the influence of light on the treatment of nitrobenzene (NB) in aqueous solutions. Three different experimental devices were used to perform a detailed study: a photoreactor with four low-pressure mercury lamps ($\lambda = 253.7$ nm), a tubular photoreactor with a polychromatic Xe lamp ($290 < \lambda < 1200$ nm), and finally a solar reactor (sunlight). TOC analyses were performed in order to monitor and compare the extent of these processes, each of them being performed with one of the three different sources of light. The influence of Fe(II), Fe(III), H_2O_2, and light on the mineralization of NB in aqueous solutions was also studied. The successful use of sunlight as a source of energy and its effectiveness regarding Fenton processes as well as direct photolysis in the treatment of NB are presented.

Keywords: Photo-Fenton; Direct photolysis; Ultraviolet radiation; Solarbox; Solar radiation

1. Introduction

In recent years, photochemical and photocatalytic methods for the destruction of organic pollutants in wastewater have been developed. According to the literature, oxidative degradation using these treatments may reach complete mineralization of the organic contaminants [1,2]. Nitroaromatic compounds are widely used in the production of different kinds of products, such as explosives and pesticides. Many of them, including nitrobenzene (NB) and all nitrophenols, are considered highly toxic compounds [3]. Purification of wastewater contaminated with these pollutants is very difficult, since they are usually resistant to microbial degradation.

The use of UV-visible light with the aid of an oxidant like hydrogen peroxide or ozone has been utilized successfully for the destruction of hazardous organic substances in water containing nitro compounds [3–8]. However, a detailed study on the influence of the type of light used has not yet been performed. By using H_2O_2, ferrous or ferric salts and UV-visible light, hydroxyl radicals ($HO^\bullet$) can be very effectively generated via the following key steps [9]:

$$Fe^{2+} + H_2O_2 \rightarrow Fe^{3+} + HO^\bullet + HO^- \quad (1)$$

$$H_2O_2 \xrightarrow{h\nu} 2HO^\bullet \quad (2)$$

$$Fe^{3+} + H_2O \xrightarrow{h\nu} Fe^{2+} + HO^\bullet + H^+ \quad (3)$$

* Corresponding author. Tel.: +34-93-4021290; fax: +34-93-4021291.
E-mail address: esplugas@angel.qui.ub.es (S. Esplugas).

0920-5861/02/$ – see front matter
PII: S0920-5861(02)00227-4

More equations are involved in the mechanism of hydroxyl radical generation, but the above cited are the most significant. The versatility of the advanced oxidation processes (AOPs) is also enhanced by the fact that they offer different possible ways to produce hydroxyl radicals, thus allowing better compliance with the specific treatment requirements. The involvement of many additional free-radical reactions in the Fenton process has been discussed extensively in the literature [10]. Moreover, Fe^{4+} has been proposed as the main reactive intermediate apart from $HO^{\bullet}$ [11]. For the best possible performance, the pH was set to values between 2.7 and 3.0, which correlates with the values suggested in the literature (2.6–3.0) [11]. At higher pH values, ferric ions are likely to form insoluble hydroxide complexes. The main compounds absorbing light in the Fenton system are ferric ion complexes, e.g. $[Fe(OH)]^{2+}$ and $[Fe(RCO_2)]^{2+}$, which produce additional Fe(II) by following photo-induced, ligand-to-metal charge-transfer reactions [12] (Eqs. (4) and (5)):

$$[Fe^{3+}(OH)^{-}]^{2+} \xrightarrow{h\nu} Fe^{2+} + HO^{\bullet} \ (\lambda < \text{ca. } 450\,\text{nm}) \quad (4)$$

$$[Fe^{3+}(RCO_2)^{-}]^{2+} \xrightarrow{h\nu} Fe^{2+} + CO_2 + R^{\bullet} \ (\lambda < \text{ca. } 500\,\text{nm}) \quad (5)$$

Additionally, Eq. (4) yields $HO^{\bullet}$ radicals, while Eq. (5) results in a reduction of the total organic carbon (TOC) content of the system due to the decarboxylation of organic acid intermediates. It is very important to note that both the reactions form the ferrous ions required for the Fenton reaction (Eq. (1)). The overall degradation rate of organic compounds is considerably increased in the photo-Fenton process, even at a lower concentration of iron salts present in the system [9]. Although in the photo-Fenton process, the energy requirement is reduced and it is highly effective in the treatment of NB solutions, its application would not completely replace a more economical treatment, such as biological degradation [13,14], when possible. Thus, the photo-Fenton process could be used for pretreatment of recalcitrant compounds in order to improve treatment efficiency and assure their biocompatibility. For this pretreatment, sunlight may be applied, thereby reducing energy costs and favoring the environment.

For the development of effective wastewater treatment methods, the mineralization of contaminants into harmless end products (CO_2) is important. Therefore, during the entire reaction period, TOC is one of the most essential parameters monitored for verification of the degree of mineralization.

In this work, the mineralization of NB by means of a photo-Fenton process has been investigated using Fe(II) and Fe(III) as catalysts. UV and sunlight were applied in order to determine the effectiveness of the corresponding processes.

2. Experimental

All the experiments were carried out in three different devices: a tubular photoreactor, a solarbox with a tubular reactor and a solar reactor. The systems were operated in batch mode, and the aqueous solutions of NB were continuously re-circulated through the reactors. Actinometry experiments based on the photochemical decomposition of oxalic acid in the presence of uranyl nitrate [15,16] were performed in order to determine the photon flow entering the tubular reactor and the solarbox.

2.1. Tubular photoreactor

This reactor consists of a cylindrical quartz tube having a length of 100 cm, an external diameter of 2.2 cm and an internal diameter of 1.85 cm. It is surrounded by four 15 W low-pressure, air-cooled Hg-lamps ($\lambda = 253.7$ nm) placed parallel to its axis (Fig. 1). The measured photon flow entering the reactor, was 19.4 μeinstein s^{-1}. Because NB is highly absorbent at 254 nm, the photon flow absorbed per unit of reaction volume at this wavelength (sometimes defined as volumetric intensity) is 72 μeinstein $s^{-1}\,l^{-1}$. The 2.5 l sample was treated at a recirculation flow rate of 100 l h^{-1}. The temperature of the solution was regulated to 25 °C.

2.2. Solarbox

The solarbox is a commercial solar simulator from Cofomegra (Milano, Italy). The quartz reactor is a cylinder providing a length of 26 cm with an inner diameter of 2.1 cm and an outer diameter of 2.5 cm.

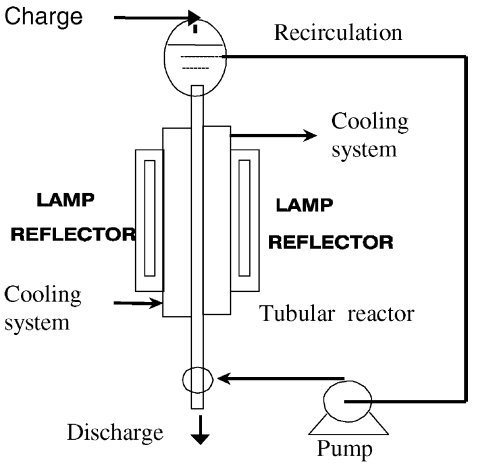

Fig. 1. Tubular photoreactor.

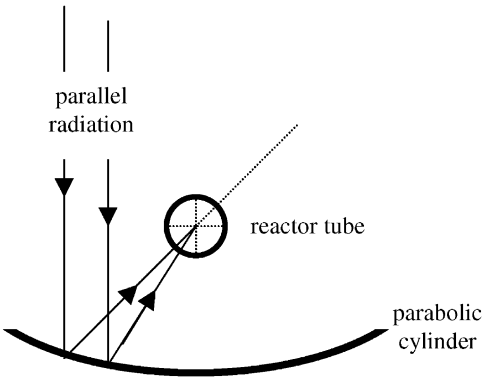

Fig. 3. Model of radiation impact.

The reactor volume is 90 cm^3. The source of radiation is a 1500 W Xenon lamp (Philips, XOP 15-OF, 290 nm $< \lambda <$ 1200 nm). A parabolic reflector is installed at the bottom providing an effective reflecting surface of 0.054 m^2 (Fig. 2). The temperature is regulated to 25 °C by circulating a water stream through a thermostatic bath. The 1.5 l volume is treated at a recirculation flow rate of 100 l h^{-1}.

In order to evaluate the radiation field inside the photoreactor, a very simple model was used. Assuming a perfect parabolic form of the reflector under the precondition that all rays strike the curve mirror surface in parallel (Fig. 3), it is assured that the entire impact of radiation is concentrated in the focus. This means that any ray passes the surface of the tube vertically, which consequently avoids significant reflection and simultaneously permits any photon to go through the entire diameter d of the tube. Because of the dimensions of the surface of the reactor and the reflector, direct radiation to the reactor was neglected.

In order to describe the absorption properties, the following equation was used:

$$\frac{W_{abs}}{W_e} = 1 - \exp(-\mu d) \quad (6)$$

To solve this equation, absorbance μ, which can easily be obtained from the absorption spectrum of NB

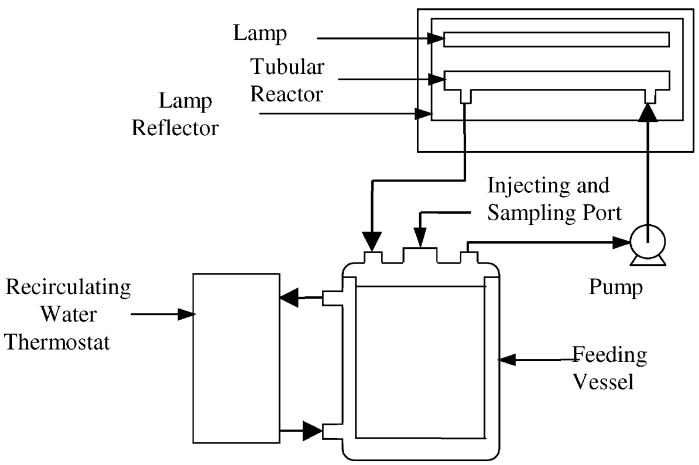

Fig. 2. Solarbox reactor.

Table 1
Flow rate of photons absorbed by NB in the solarbox reactor

Wavelength (nm)	μ (cm^{-1})	W_e (μeinstein s^{-1})	W_{abs}/W_e	W_{abs} (μeinstein s^{-1})
290	10.1	0.00112	1	0.00112
300	6.70	0.00482	1	0.00482
310	4.07	0.0106	1	0.0106
320	2.35	0.0178	0.993	0.0176
330	1.40	0.0247	0.948	0.0234
340	0.974	0.0311	0.871	0.0271
350	0.748	0.0390	0.792	0.0308
360	0.592	0.0462	0.711	0.0329
370	0.464	0.0545	0.622	0.0339
380	0.359	0.0643	0.529	0.0340
390	0.291	0.0757	0.457	0.0346
400	0.249	0.0837	0.407	0.0341

(see Fig. 5), must be calculated. Average values for μ have been inserted in Table 1. Thus, for each wavelength, the dependency between the energy flow entering the reactor (W_e), which has been measured by actinometry, and the absorbed energy flow (W_{abs}) used for the degradation process, can be calculated by means of Eq. (6). The resulting term allows the calculation of the absorbed energy flow at the starting time.

The radiation flow in the reactor absorbed by NB within the wavelength range 280 nm $< \lambda <$ 400 nm, was 0.285 μeinstein s^{-1} (equal to the sum of the emission in this spectrum, compare Table 1). This value corresponds to the starting time, when NB concentration is maximum. The photon flow absorbed by NB decreases with irradiation time, as does its concentration. Taking into account the reactor volume, the flow of photons absorbed by unit of reaction volume is 3.12 μeinstein s^{-1} l^{-1}.

2.3. Solar reactor

This prototype was designed based on a parabolic concentrator (PTC) photoreactor. The solution goes through a tubular reactor placed in the focus of a parabolic reflector. This kind of medium-concentrating solar collector concentrates sunlight between five and 50 times, and usually requires continuous tracking of the sun's movement [17,18]. In our case, this was done manually. The cylindrical reactor strongly resembles the reactor used in the solarbox (see Fig. 2). It also has a length of 26 cm and a diameter of 2.1 cm. The dimensions of the reflector are 32 cm × 54.5 cm (0.174 m^2), whereby, for design reasons, only half of the surface (0.087 m^2) can be considered reflecting in so far as surface supplying the process with photons. Again, the treated volume is 1.5 l at a recirculation flow rate of 100 l h^{-1}(Fig. 4).

As with the solarbox, a perfect parabolic form of the reflector surface was assumed. Therefore, the same assumptions can be made: the rays enter vertically into the tube and are concentrated onto the focus. Since actinometry has not yet been carried out, the radiation entering the reactor was set equal to the direct solar radiation emitted. Unlike the solarbox, the sun's characteristics change, obviously, according to the meteorological conditions. Therefore, a generally valuable calculation cannot be provided. For a cloudless day providing a remarkable amount of direct radiation (21 June 2001), the energetic intensities for each wavelength of interested were calculated with the aid of STAR (software for the prediction of radiation, developed under the lead of the Meteorological Institute at the University of Munich, Germany). Thus, the entering energy W_e may be estimated, as shown in Table 2. With the aid of Eq. (6), the flux of absorbed energy (W_{abs}) was calculated. The photon flow entering the reactor within the wavelength range 300 nm $< \lambda <$ 400 nm calculated was 9.86 μeinstein s^{-1} (see Table 2). The corresponding absorbed photons flow per unit of reaction volume is 109 μeinstein s^{-1} l^{-1}, which is the highest value, assuming a reflector efficiency of 100%.

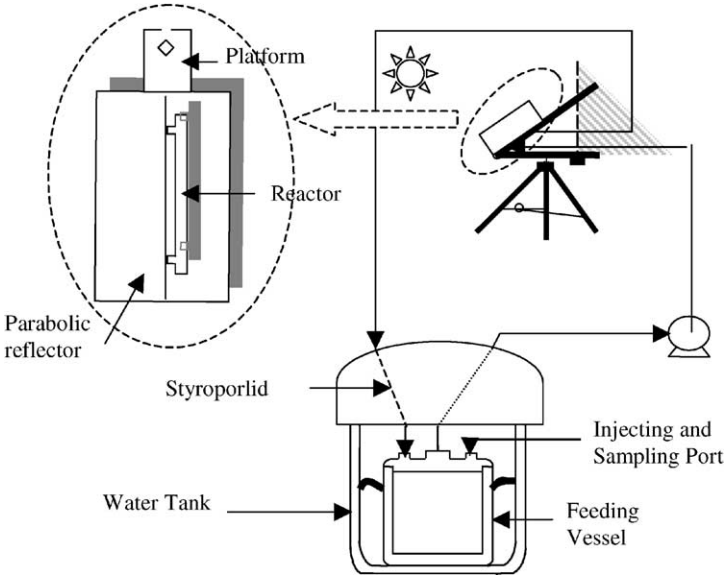

Fig. 4. Solar reactor.

2.4. Reactives

NB (99% pure, Probus), phosphoric acid (85% pure, Probus), sulfuric acid (95–97% pure, Fluka), oxalic acid (99.5% pure, Panreac), uranyl nitrate (98% pure, Panreac), hydrogen peroxide (30% pure, Merck), $FeSO_4{\cdot}7H_2O$ (98% pure, Panreac), $FeCI_3{\cdot}6H_2O$ (98% pure, Probus), $Fe(NO_3)_3{\cdot}9H_2O$ (99% pure, Merck), and sodium hydrogen sulfite solution (40% (w/v) pure, Panreac) were used as received. Stock solutions of all reagents were prepared in millipore water (Milli-Q Millipore system with a 18 $M\Omega\,cm^{-1}$ resistivity).

2.5. Analysis

TOC was monitored during the mineralization of the aromatic compounds by means of a TOC analyzer (Rosemont Dohrmann DC-190). The pH of the reaction solution was measured with a Crison GLP 22 pH meter. The consumption of H_2O_2 in solution

Table 2
Photons flow absorbed by NB in the solar reactor

Wavelength (nm)	μ (cm^{-1})	W_e (μeinstein s^{-1})	W_{abs}/W_e	W_{abs} (μeinstein s^{-1})
290	10.1	0.000001	1	0.000001
300	6.70	0.00507	1	0.00507
310	4.07	0.163	1	0.163
320	2.35	0.641	0.993	0.636
330	1.40	1.20	0.948	1.13
340	0.974	1.33	0.871	1.15
350	0.748	1.65	0.792	1.31
360	0.592	1.72	0.711	1.22
370	0.464	2.01	0.622	1.25
380	0.359	2.07	0.529	1.10
390	0.291	1.92	0.457	0.880
400	0.249	2.64	0.407	1.07

was monitored by means of a Merkoquant (Merck) and Quantofix (Macherey-Nagel) peroxide test in the range 0.03–3 mmol l^{-1}.

2.6. Experimental operation

The photoreactors were always charged with aqueous solution of 0.82 mmol l^{-1} of NB. Sulfuric acid was used for the adjustment of the pH to the range 2.7–3.0. At various intervals, samples of the reaction solution were withdrawn from the reactor during the mineralization experiments. The samples were tested for consumption of H_2O_2 and were used for the TOC analysis after being quenched with sodium hydrogen sulfite solution in order to avoid further reactions.

3. Results and discussion

Previous experiments had been carried out to exclude the effect of vaporization or stripping of NB. In these experiments absolutely no change in NB concentration by HPLC analysis. Table 3 shows the experiments carried out in the three different devices described above. Note that, as mentioned, in all the experiments the initial concentration of NB was 1.14 mmol l^{-1}, the pH was set to the values of about 3.0, and the temperature range was variable depending on the reactor used.

Table 3
Experimental conditions

Run	Reactor	$[H_2O_2]_0$ (mmol l^{-1})	$[Fe(III)]_0$ (mmol l^{-1})	$[Fe(II)]_0$ (mmol l^{-1})
NB1	Tubular	0	0	0
NB2	Tubular	0	1.07	0
NB3	Tubular	21.3	0	0
NB4	Tubular	21.3	1.07	0
NB5	Tubular	42.7	1.07	0
NB6	Tubular	42.7	0	1.07
NB7	Solarbox	0	0	0
NB8	Solarbox	21.3	1.07	0
NB9	Solarbox	0	1.07	0
NB10	Solarbox	21.3	0	0
NB11	Solarbox	21.3	0	1.07
NB12	Solar reactor	0	0	0
NB13	Solar reactor	0	0	0
NB14	Solar reactor	21.3	0	1.07
NB15	Solar reactor	10.6	0	1.07
NB16[a]	Solar reactor	21.3	0	1.07
NB17	Solar reactor	42.7	0	1.07
NB18	Solar reactor	0	0	1.07
NB19	Solar reactor	0	1.07	0
NB20	Solar reactor	10.6	0	0
NB21	Solar reactor	21.3	0	0
NB22	Solar reactor	21.3	0	0.54
NB23	Solar reactor	21.3	0	2.14
NB24	Solar reactor	21.3	0.54	0
NB25	Solar reactor	21.3	1.07	0
NB26	Solar reactor	42.7	2.14	0
NB27	Solar reactor	10.6	1.07	0
NB28	Solar reactor	42.7	1.07	0.54

[a] Cloudy day.

3.1. Absorption properties of important compounds

The peak of the NB absorption curve at 263 nm (Fig. 5) should be pointed out. Furthermore, NB shows the capacity to absorb in higher wavelength ranges up to ~400 nm. On the contrary, quasi H_2O_2 does not absorb at wavelengths above 300 nm. The graphs are comparable because the ratio H_2O_2/NB was set to the usual value for the experimental reactions.

3.2. Direct photolysis

Fig. 6 shows the influence of the different types of light: UV 254 nm, xenon light (solarbox) and solar light, on direct photolysis of NB. By direct illumination of the aqueous solutions, organic radicals are generated for the photolysis of the substrates. These radical intermediates are subsequently trapped by dissolved molecular oxygen and lead, via peroxyl radicals ($ROO^{\bullet}$), to an enhancement of the overall degradation process. Finally a mineralization grade of up to 76% was reached. Moreover, the absorption spectrum of the aqueous solutions of NB extends into the lower-energetic UV region of the solar spectrum (UV-A, see Fig. 5). Since the parameter μ of the equation (see Table 2) is directly proportional to the absorption characteristics, NB is able to perform a remarkable absorption of photons below 400 nm. It is obvious that even high wavelengths (>250 nm) contribute to the total absorption of NB in a notable manner. Consequently, photoalteration processes of the NB molecules can occur. This fact could help to explain the high effectiveness of direct photolysis in the mineralization of NB solutions. The results indicate that within 2 h, the mineralization of NB is 53.3, 59.6 and 76.2% for irradiation with UV (253.7 nm),

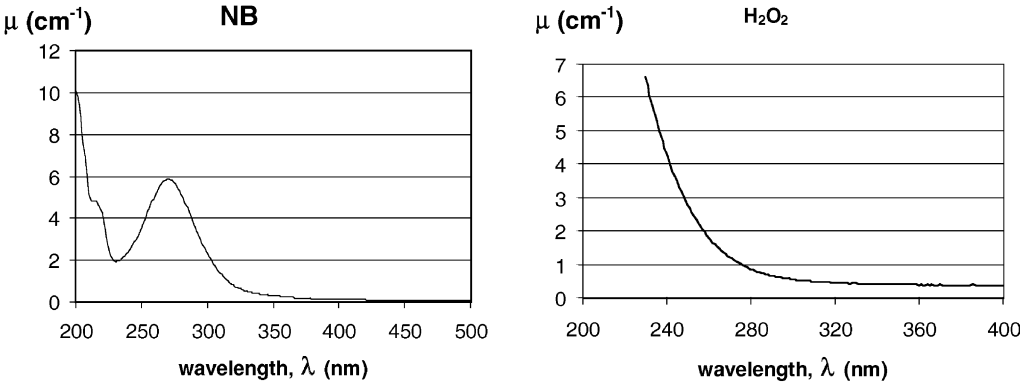

Fig. 5. Absorption spectrum of NB (0.82 mmol l^{-1}) and H_2O_2 (10.6 mmol l^{-1}).

solarbox and solar light, respectively. As the dimensions of the reactor used in the solarbox and in the solar experiments are the same, and the radiation spectrum was similar, it is possible to compare the results of the solarbox and the solar light. TOC reduction was greater in the solar reactor because the absorbed photons flow per unit of reaction volume was higher.

3.3. Photo-Fenton

The advantage of the photo-Fenton reaction in the mineralization of organic aqueous solutions is well known [4,19]. The addition of iron salts (photo-Fenton) to the reaction medium results in increased mineralization. As can be observed in Fig. 7, a very high degree of TOC reduction (nearly 96%) is obtained in the solar reactor in only 40 min of irradiation, if the initial concentrations of iron(III) and hydrogen peroxide are 1.07 and 2.13 mmol l^{-1}, respectively. For long irradiation times, the best results were obtained for sunlight, but the differences in TOC reduction are very small when compared to UV radiation (254 nm). However, especially at initial times, solar light (80% TOC reduction in 20 min) is more effective than UV light (50% TOC reduction in 20 min). This behavior can be explained by the fact that iron(III) is converted to $Fe(OH)^{2+}$ in aqueous solution. This complex absorbs notably in the range above 300 nm, which leads to remarkable production of hydroxyl radicals according to the following reaction [20]:

$$Fe(OH)^{2+} \xrightarrow{h\nu} Fe^{2+} + HO^{\bullet} \quad (7)$$

The necessary wavelengths of up to 365 nm are actually present in a relevant amount within the solar

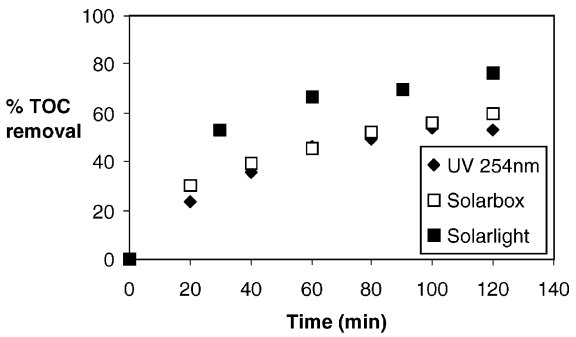

Fig. 6. Direct photolysis of NB using different light sources.

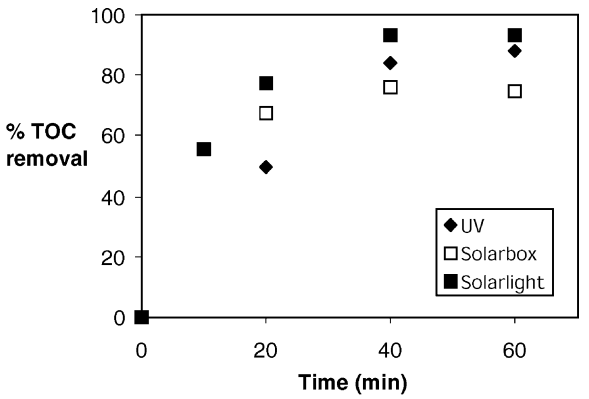

Fig. 7. Photodegradation of NB using different light sources.

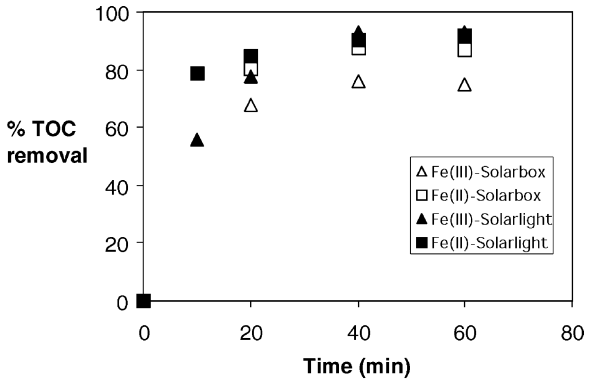

Fig. 8. Effectiveness of Fe(II) and Fe(III) on the photodegradation of NB using sunlight and solarbox.

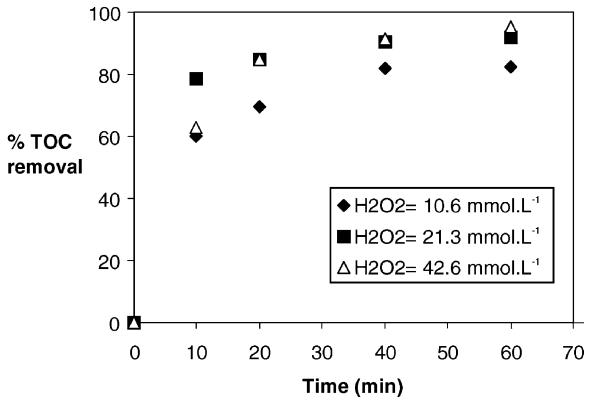

Fig. 9. Influence of H_2O_2 concentration on the photodegradation of NB using sunlight.

spectrum. Greater reductions in TOC are obtained, if iron(II) is used instead of iron(III) for the solarbox, as well as for the application of solar light. Fig. 8 shows the TOC removal for an initial concentration of iron(II) or iron(III) of 1.07 mmol l^{-1} at an initial concentration of H_2O_2 of 21.3 mmol l^{-1}. The main part of the TOC reduction takes place during the first 10 min. At startup, iron(II) is a little more effective than iron(III) due to the generally worse kinetics of iron(III) in comparison to iron(II) at the beginning of the Fenton process ($k_2 = 0.01\,l\,mol^{-1}\,s^{-1} \ll k_1 = 63\,l\,mol^{-1}\,s^{-1}$) [21,22]. A 90% TOC reduction was obtained by using iron(III) or iron(II) and sunlight.

It is interesting to compare the solar reactor and the solarbox (sunlight simulator). This difference could be explained by taking into account the effective flow of radiation entering both reactors (Section 2). Another important factor to be considered is the behavior of the temperature. Whereas in the solarbox it was regulated to 25 °C, it ranged between 25 and 35 °C in the solar reactor, since there a steady temperature control could not be established. As shown in previous work, the reaction temperature is supposed to accelerate the mineralization of diverse compounds [19,23].

The effect of initial hydrogen peroxide concentration on the TOC reduction is shown in Fig. 9. A NB solution containing 1.07 mmol l^{-1} iron(II) was treated with sunlight. It can be observed that, if the initial concentration of hydrogen peroxide increases, the TOC reduction does so also. The initial concentration of iron(II) has less influence on TOC reduction than the concentration of hydrogen peroxide. By using an initial concentration of hydrogen peroxide of 21.3 mmol l^{-1}, the final TOC reduction with the use of the sunlight is practically the same for Fe(II) concentrating ranging from 0.54 to 2.14 mmol l^{-1} (Fig. 10). Only at the start are small differences found.

Fig. 11 shows a comparison of direct photolysis, UV-hydrogen peroxide and the photo-Fenton reaction with both the types of iron, i.e. iron(II) and iron(III) for the solar reactor. The initial concentration of hydrogen peroxide is 21.3 mmol l^{-1}. The concentration of iron(II) and iron(III) are 1.07 mmol l^{-1}. The addition of iron salts (photo-Fenton) to the reaction medium leads to a great improvement of the mineralization rate. Within only 60 min, a TOC reduction of 95% is achieved for iron(II) as well as for iron(III). As already discussed in Section 3.2, the NB mineralization

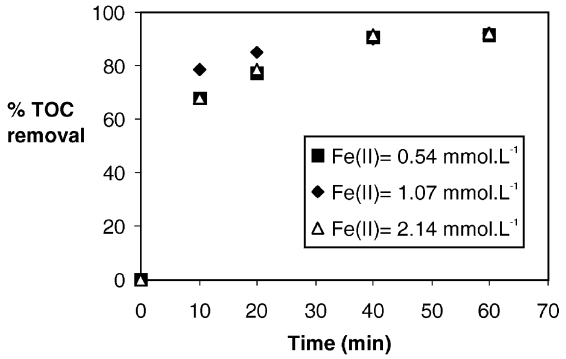

Fig. 10. Influence of Fe(II) concentration on the photodegradation of NB using sunlight.

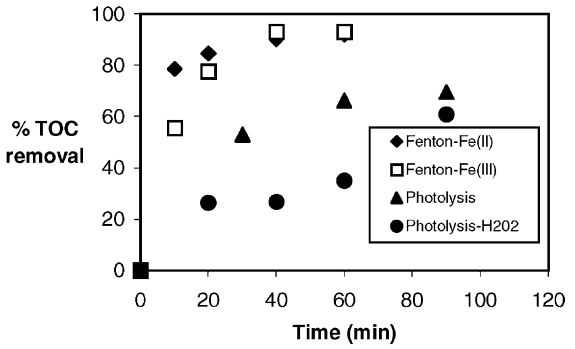

Fig. 11. Effect of direct photolysis, photo-Fenton and photolysis of H_2O_2 on the degradation of NB.

process also works fine with direct photolysis. Finally, after 90 min, this leads to a respectable mineralization of 70%, whereas the addition of hydrogen peroxide apparently worsens the reaction kinetics, especially during the initial processes. Although hydrogen peroxide does not show good absorption properties in the UV-A range, total absorption is remarkable due to the relatively high amounts of H_2O_2 in the solution, which results in a kind of competition between NB and H_2O_2 for the impacting photons. Therefore, an inhibition effect can be observed during the first phase (see Fig. 11). Finally, the mineralization rates of photolysis and H_2O_2-photolysis achieved are the same. However, the delay of H_2O_2-photolysis in the initial phase proves that it is not the H_2O_2, but the iron salts that are responsible for the increased rate of mineralization found for the photo-Fenton process.

4. Conclusions

The results indicate that, of the varied variables, sunlight provides the best mineralization of NB (nearly 95% TOC reduction) in the photo-Fenton treatment. Furthermore, iron(II) and iron(III) reached the same level of degradation with extended irradiation times. For H_2O_2-photolysis with solar light, an inhibition effect, caused by a kind of competition between NB and H_2O_2 in terms of the absorption of photons, has been detected. Consequently, the mineralization process has to suffer a delay in the initial phase. In contradiction to this behavior, the good reduction of TOC by sunlight alone (photolysis) must be underlined, since for other compounds, it is generally supposed to be inefficient.

The most important conclusion is the fact that solar light is an excellent supply of energy in terms of the decomposition of NB, for the photo-Fenton process as well as for direct photolysis, since it offers a cheap and environmentally friendly source of energy.

Acknowledgements

The authors wish to express their gratitude for the economic support given by the Spanish Ministry of Education and Culture (CICYT projects AMB 98-0357, 99-0442 and PPQ2001-3046) and the Generalitat de Catalunya (project SGR-00298). M. Rodriguez expresses his gratitude to the ULA-CONICIT (Venezuela) agreement. V. Timokhin thanks the Spanish Ministry of Education and Culture for the NATO Science Fellowship.

References

[1] J. Sarasa, P. Roche, P. Ormad, E. Gimeno, A. Puig, J.L. Ovelleiro, Water Res. 32 (1998) 2721.
[2] O. Legrini, E. Oliveros, A.M. Braun, Chem. Rev. 93 (1993) 671.
[3] E. Lipczynska-Kochany, Chemosphere 22 (1991) 529.
[4] E. Lipczynska-Kochany, Chemosphere 24 (1992) 1369.
[5] M. Rodriguez, A. Kirchner, S. Contreras, E. Chamarro, S. Esplugas, J. Photochem. Photobiol. A 133 (2000) 123.
[6] F.J. Beltran, J.M. Encinar, M.A. Alonso, Ind. Eng. Chem. Res. 37 (1998) 32.
[7] S. Contreras, M. Rodriguez, E. Chamarro, S. Esplugas, J. Photochem. Photobiol. A 142 (2001) 79.
[8] W.H. Glaze, J.W. Kang, D.H. Chapin, Ozone Sci. Eng. 9 (1987) 335.
[9] R. Chen, J.J. Pignatello, Environ. Sci. Technol. 31 (1997) 2399.
[10] J. de Laat, H. Gallard, S. Ancelin, B. Legube, Chemosphere 39 (1999) 2693.
[11] J.J. Pignatello, Environ. Sci. Technol. 26 (1992) 944.
[12] G. Sagawe, A. Lehnard, M. Lubber, D. Bahnemann, Helv. Chim. Acta 84 (2001) 3742.
[13] C. Pulgarin, M. Invernizzi, S. Parra, V. Sarria, R. Polonia, P. Peringer, Catal. Today 54 (1999) 341.
[14] S. Parra, V. Sarria, S. Malato, P. Perengir, C. Pulgarin, Appl. Catal. B 27 (2000) 153.
[15] D.H. Volman, J.R. Seed, J. Am. Chem. Soc. 86 (1964) 5095.

[16] L.J. Heidt, G.W. Tregay, F.A. Middleton, J. Phys. Chem. 74 (1979) 1876.
[17] J. Blanco, S. Malato, Proceedings of the Sixth International Symposium on Solar Thermal Concentrating Technology, Mojacar, Spain, CIEMAT, Madrid, 1992.
[18] J. Blanco, S. Malato, in: D. Ollis, H. Al-Ekabi (Eds.), Photocatalytic Purification and Treatment of Water and Air, Elsevier, Amsterdam, 1993, p. 639.
[19] R. Bauer, G. Waldner, H. Fallmann, S. Hager, M. Klare, T. Krutzler, S. Malato, P. Maletzky, Catal. Today 53 (1999) 131.
[20] P. Mazellier, M. Bolte, Chemosphere 42 (2001) 361.
[21] J. de Laat, H. Gallard, Environ. Sci. Technol. 33 (1999) 2726.
[22] S. Lin, M. Gurol, Environ. Sci. Technol. 32 (1998) 1417.
[23] M. Rodriguez, V. Timokhin, S. Contreras, E. Chamarro, S. Esplugas, Adv. Environ. Res., in press.